

GT2011-45198

TOWARDS SURROGATE REACTION MODEL DEVELOPMENT

N.A. Slavinskaya

A. Zizin

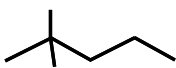
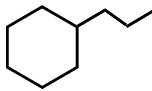
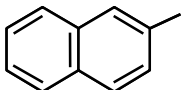
U. Riedel

German Aerospace Center (DLR) Institute of Combustion Technology
 Stuttgart, Germany

ABSTRACT

The present paper describes the proposed strategy of fuel model design based on identification of chemical *and* physical criteria for the selection of initial formula of the reference fuel. The first 8 criteria established and studied in previous papers so far are combustion enthalpy, formation enthalpy, molecular weight, C/H-ratio, sooting tendency index, critical point, two-phase diagram, and distillation curve. With these criteria established, the following candidate formula of the kerosene surrogate blend is defined and optimized to adequately mimic the properties of the real fuel: 10% n-propylcyclohexane, 13% iso-octane, 20% n-dodecane, 23% 1-methylnaphthalene, and 32% n-hexadecane. In this work, the ignition delay time has been studied as the next optimization criterion. To keep the model size small, the core reaction mechanism - the skeletal kinetics of n-heptane and iso-octane combustion including aromatics formation, developed earlier - is extended by n-propylcyclohexane, 1-methylnaphthalene, n-dodecane, and n-hexadecane sub-models. The lumped mechanisms for larger n-alkanes are constructed in a similar way to that for n-decane. The n-propylcyclohexane oxidation sub-model is derived from a skeletal mechanism for the low and high temperature cyclohexane oxidation. Reactions for 1-methylnaphthlene oxidation are included in the sub-mechanism for the formation of aromatics up to 5 ringed molecules. The mechanism includes 189 species and 1125 reactions. The proposed sub-models and overall mechanism are validated against experimental data obtained in shock tubes and in jet stirred reactor.s The simulations of ignition delay data for all hydrocarbons and their mixtures, i.e. for kerosene, are in good agreement with the measured data.

NOMENCLATURE

Iso-octane, i-C ₈ H ₁₈	
Dodecane, C ₁₂ H ₂₆	$\text{CH}_3 - \left(\overset{\text{H}_2}{\underset{\text{C}}{\text{---}}} \right)_{10} - \text{CH}_3$
Hexadecane, C ₁₆ H ₃₄	$\text{CH}_3 - \left(\overset{\text{H}_2}{\underset{\text{C}}{\text{---}}} \right)_{14} - \text{CH}_3$
Propyl-cyclohexane, cyC ₉ H ₁₈	
Methylnaphthalene, A2CH ₃ (C ₁₁ H ₁₀)	

INTRODUCTION

Numerical combustion modeling is an essential and effective tool for combustion chamber design. Unfortunately, it is currently not possible to represent the complex chemistry of real fuel in a detailed chemical kinetics model: practical fuels, such as gasoline, kerosene, diesel, etc. are complex mixtures of several hundreds of individual species. The kinetics of all of the components and kinetics interactions among them are not

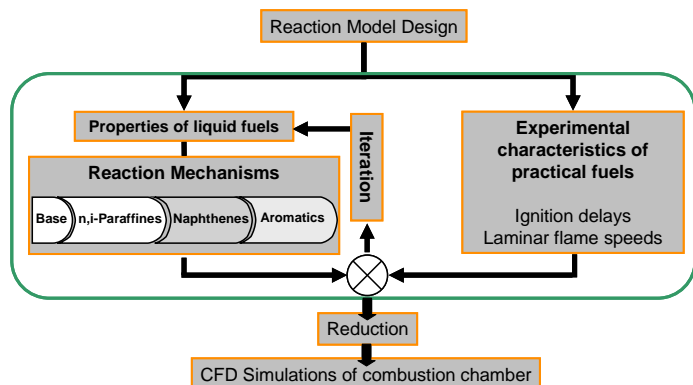


Figure 1. The principle scheme for design of the practical fuel reaction model.

fully determined. Moreover, the numerical CFD-tools used in combustion simulations do currently not have the capabilities to use comprehensive chemical models. Therefore, only simplified reaction models of practical fuels - surrogate blends or reference fuels, which represent the real fuels chemical kinetics with a small number of pure components - can be used presently in the design of combustion chambers. In order to determine the optimal composition for a surrogate blend, which mimics the real fuel combustion properties, one needs to specify criteria for choosing appropriate surrogate candidates. The set of relevant criteria for a particular surrogate fuel should be determined through chemical *and* physical properties, combustion chamber characteristics and operating conditions [1, 2]. Identifying relationships between fuel chemical composition and fuel properties and performance is the predominant concern of Reaction Model Design (RMD) for real fuels.

A large number of surrogate fuel mixtures, well described in the review [3], have been proposed recently, evaluated in engines, in fundamental experiments, and studied numerically. Most of those were developed for various jet fuels [3 - 5]. These models simulate the fuel oxidation chemistry and generally successfully reflect the combustion kinetics. Unfortunately, the capabilities of the surrogate models to reflect *joint requirements for chemical and physical properties* are considerably less studied [6].

The present paper aims at the development of chemical kinetics mechanisms for kerosene surrogate with the Input Formula of Surrogate (IFS) obtained from the optimization of universal characteristics of the fuel, Fig.1. The following properties of liquid fuel are considered in specifying the surrogate blend: combustion enthalpy, formation enthalpy, molar weight, C/H ratio, sooting tendency index, critical point, two phase diagram,

Table 1. Content of studied reference blend and its main physical properties.

10% - $\text{cyC}_9\text{H}_{18}$	Combustion enthalpy $\Delta_c H_f$	45 MJ/kg
+ 13% - $\text{i-C}_8\text{H}_{18}$	Formation enthalpy ΔH_f	-160 kJ/mol
+ 20% - $\text{C}_{12}\text{H}_{26}$	Molar weight	145 g/mol
+ 25% - $\text{C}_{11}\text{H}_{20}$	Approximate formula	$\text{C}_{11}\text{H}_{19}$
+ 32% - $\text{C}_{16}\text{H}_{34}$	Sooting Tendency Index	27.8

and distillation curve. These criteria stem from the approach that combustor hardware such as injectors and heat exchangers ultimately provide criteria for the design of higher-performing fuels for current and future engine systems. As the evaporation characteristics is very important for the pre-combustion processes in injectors, i.e. fuel atomization, evaporation and mixing, special attention has to be given to the simulation of the two-phase diagram of fuels. The numerical code based on the cubic equation of state (Soave modification of Redlich-Kwong equation of state) and Van der Waals mixing rule has been elaborated for calculation of phase diagrams, critical points and distillation curves of multi-component mixtures of hydrocarbons [6]. In [6] the hydrocarbons used in different chemical models for gasoline, kerosene and diesel are summarized and the resulting mixture derived from optimization of the 8 criteria, Fig. 2, described above is given. The optimized blend includes adequate fractions of different chemical families of fuels (primarily paraffins, naphthenes(cycloparaffins), and aromatics). It consists of n-propylcyclohexane ($\text{cyC}_9\text{H}_{18}$), iso-octane ($\text{i-C}_8\text{H}_{18}$), n-dodecane ($\text{n-C}_{12}\text{H}_{26}$), 1-methylnaphthalene (A2CH_3), and n-hexadecane ($\text{n-C}_{16}\text{H}_{34}$). This mixture containing 5 components in the IFS is practically manageable, has the main properties of kerosene [7], Table 1, and closely matches the boiling-point curve and the two-phase diagram for Jet-A, Fig.2.

To test the chemical properties of the proposed surrogate reaction models for each individual hydrocarbon in the surrogate blend have to be generated to simulate the chemical properties of the fuel.

In this paper, ignition delay times have been selected as the 9th criterion for further IFS validation.

For that kinetic sub mechanisms for $\text{cyC}_9\text{H}_{18}$, $\text{n-C}_{12}\text{H}_{26}$, A2CH_3 and $\text{n-C}_{16}\text{H}_{34}$ have been developed as the extension of the overall reaction mechanism of larger hydrocarbons C_7H_8 , $\text{n-C}_7\text{H}_{16}$, $\text{i-C}_8\text{H}_{18}$, and $\text{n-C}_{10}\text{H}_{22}$, [8 - 11]. This kinetic mechanism has a strong hierarchical structure and is developed as continual data base of chemical kinetic data for hydrocarbons. The new sub models have been developed by applying global sensitivity analysis, linear lumping and simplification procedures. This allowed decreasing the complexity of the full model without losing significant chemical details. The obtained this way kerosene reaction model is useful for the global reduction to be

run in CFD modeling. The core mechanism for smaller hydrocarbons is based on careful analysis and proper definition of the species and reactions involved [8 - 10].

The new sub-models proposed and reference mixtures have been validated against ignition delay data from shock tube experiments and species concentration profiles measured in jet-stirred reactors (JSR) [13 – 19], Table 2.

Table 2. Experimental data used for model validation

Sub Mechanism	Ignition delay	JSR
cyC ₉ H ₁₈ /air	$p = 1.0 - 1.7$ atm $T_5 = 1250 - 1820$ K $\phi = 0.5 - 1.5$ [13]	
n-C ₁₂ H ₂₆ /air	$p = 18 - 33$ atm $T_5 = 700 - 1200$ K $\phi = 0.5 - 1.0$ [14]	
A2CH ₃ /air	$p = 13.0$ atm $T_5 = 1000 - 1335$ K $\phi = 1.0$ [16]	
n-C ₁₆ H ₃₄ /air		$p = 1.0$ atm $T_o = 1000 - 1200$ K $\phi = 1$, $\tau = 70$ ms [15]
Jet A = cyC ₉ H ₁₈ + i-C ₈ H ₁₈ + n-C ₁₂ H ₂₆ + A2CH ₃ + n-C ₁₆ H ₃₄	$p = 7.7 - 25.0$ atm $T_5 = 874 - 1929$ K $\phi = 0.5 - 2$ [18, 19]	

MECHANISM GENERATION

The general approach to develop reduced reaction mechanism for surrogate fuel blends is based on the implementation of a minimal set of new components, elementary and lumped reactions in the core detailed kinetic mechanism and the concatenation of sub-mechanisms to the overall mechanism. The reaction model for n-heptane (n-C₇H₁₆) and iso-octane [8, 9], elaborated earlier, has been used as the core detailed reaction model. This model is based on profound investigations [20 - 23], which yielded detailed information about the properties of the reaction mechanisms for low and high temperature oxidation of large hydrocarbons. Further this model has been extended by a mechanism describing poly-aromatic hydrocarbon (PAH) formation, including toluene (C₇H₈) oxidation [10], and in a subsequent step by n-decane (n-C₁₀H₂₂) oxidation sub-mechanism [10,11]. This base chemistry of the surrogate mechanism was carefully validated [8 - 11] for

- ignition delay times of pure C₇H₈, n-C₇H₁₆, i-C₈H₁₈, and n-C₁₀H₂₂, and their mixtures
- laminar flame speed for C₇H₈, n-C₇H₁₆ and n-C₁₀H₂₂

- concentration profiles of small and aromatic molecules as well as soot in premixed laminar CH₄, C₂H₄, n-C₇H₁₆/air/O₂ flames.

Experimental data used for model validations cover the

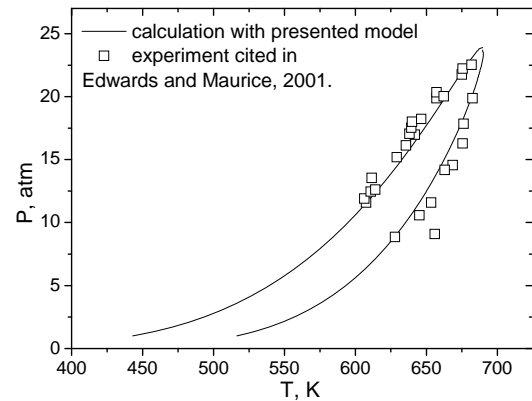


Figure 2. Calculated phase diagram for the proposed fuel surrogate compared to experimental data cited in [7] for Jet-A.

parameter range 0.5 - 2 for equivalent ratios, 700 – 1400 K for initial temperatures and 1.0 – 55.0 atm for initial pressures.

The global sensitivity analysis implemented in the in-house developed RedMaster code [11] has been applied to reduce the basic mechanism to the skeletal one. The multi target reduction strategy realized in the RedMaster code, Fig.3, allows determination and elimination of unimportant species and reactions on the basis of integrated information obtained from the mechanism sensitivity analysis performed for different fuels, different processes (presently ignition delay time and laminar flame simulations) and different time points of the studied processes.

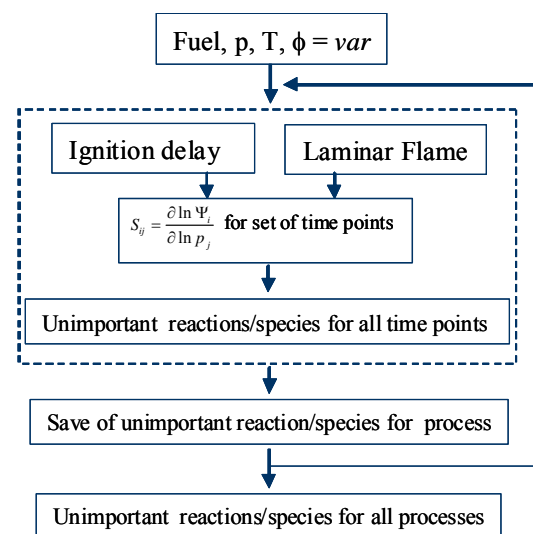


Figure 3. Principal scheme of the RedMaster code for the multi target reaction mechanism reduction

This tool is capable to

- start CHEMKIN calculations of ignition delays for a group of selected experimental data automatically
- choose the appropriate type of sensitivity analysis and calculate corresponding sensitivity coefficients
- select automatically the time points for which a sensitivity analysis will be performed
- select reactions and species commonly unimportant for all studied time points of the process
- accumulate the information about all unimportant reactions (species) for all selected experimental data
- eliminate the reactions (species) from a model which are unimportant simultaneously for all simulated processes and to produce a ready-to-use reduced mechanism.

The elaborated automatic tool uses classical sensitivity methods for reaction scheme analysis. A species may be considered redundant if its concentration change has no significant effect on the production rate of important species. The influence of a change of the concentration of species j on the rate of production of a p -membered group of important species i , can be calculated as the sum of squares of the *overall normalized sensitivity coefficient* [24]

$$B_j = \sum_i^p \left(\frac{\partial \ln R_i}{\partial \ln c_j} \right)^2 \quad (1)$$

B_j yields the effect of a change of the concentration of species c_j on the rate of production of species i , R_i , from a group of p important species, $i = 1, 2, \dots, p$; p is the number of important species given by the investigator on the first step of the analysis. The value of B_j defines the direct effect of species j , on the species i . As there are necessary species which influence the concentration of important species not through a direct coupling but through their influence on "primary" necessary species, the group of necessary species has to be identified by an iterative procedure: after each step of B_j calculation only one species with the greatest value B_j is added to the group of important and necessary species. After the last iteration, those species which were added to the first main group at the last iterations can be considered as redundant species.

The contribution of reaction steps to the production rate is based on the sensitivity of production rates to changes in rate parameters. The effect of changing the reaction rate coefficient k_i on the rate of production of species i , R_i , in a mechanism with N species is calculated as the sum of squares of the *overall normalized sensitivity coefficient* [24]

$$A_i = \sum_j^N \left(\frac{\partial \ln R_j}{\partial \ln k_i} \right)^2 \quad (2)$$

R_j - the rate of production of species j , k_i - rate coefficient of reaction i . A reaction i is considered important if its coefficients A_j , calculated as the sum for all species, e.g. N , are larger than a pre-defined threshold value Δ .

A reduction cycle has to be repeated several times until the simulations with the resulting reduced mechanism reveal that the results achieved fulfil the pre-defined agreement requirement with experimental data.

Thus, it is made possible to create a skeletal model, which keeps the capabilities of individual sub-mechanisms and overall surrogate model.

For the core mechanism reduction, 240 experimental points (see [10] for details) have been analyzed: 235 ignition delay data for C_7H_8 , $n-C_7H_{16}$, $i-C_8H_{18}$, and $n-C_{10}H_{22}$; three flame speed calculations for $n-C_{10}H_{22}$; two simulations of PAH concentration profiles obtained in laminar premixed flames of C_7H_8 and $n-C_7H_{16}$. In the cases studied a reduced model with 118 components and 814 reactions has been obtained from detailed mechanism with 179 species and 1180 reactions without the loss of predictive capabilities for the C_7H_8 , $n-C_7H_{16}$, $i-C_8H_{18}$, and $n-C_{10}H_{22}$ sub-mechanisms.

Simplifications, analogy rules and lumping techniques have been applied to sub-models for cyC_9H_{18} , $n-C_{12}H_{26}$, A_2CH_3 and $n-C_{16}H_{34}$ to reduce the reaction pool to a set of reference reactions and to restrict long-chained radicals and intermediate molecules directly to smaller radicals and molecules already existing in the core model. For that, first, reactions of relatively heavy radicals have been neglected for the following reasons: (a) rate constants for reactions of radical addition, H abstraction and chain-termination with large radicals decrease with increasing number of C atoms in the molecule; (b) rate constants for reactions of internal isomerisation and decomposition increase with increasing number of C-atoms in the molecule that yield smaller radicals and unsaturated molecules.

Second, lumping techniques has been applied [24] to isomers, equivalent components and to a cascading decomposition chemistry of olefins and alkyl radicals.

Linear lumping was used mostly to reduce the number of isomers in the model. The lumping matrix M , which transforms the vector of species y to the vector of new species \hat{y} , is

$$\hat{y} = My. \quad (3)$$

Applying linear lumping, we can always construct the lumping matrix M , and obtain the Jacobian for the lumped system from the condition

$$\hat{K} = MK\hat{M}, \text{ by } M\hat{M} = I \quad (4)$$

K is Jacobian of the input system; \hat{K} is the new Jacobian.

Given the ratios between isomer concentrations in the lumping matrix M , the rate of the resulting lumped reactions can be obtained. It is useful to choose the group of reactions for lumping on the grounds of a simplification of the matrixes

M and *K*. Of course, in simpler cases a similar lumping can be performed on the basis of experience and intuition only without application of the mathematical tools.

Third, for the generation of the sub-mechanisms a limited number of reaction classes for hydrocarbon oxidation [22] has been included. Hence, high temperature fuel consumption is described by the following sequence of steps:

- thermal decomposition of the parent hydrocarbon RH to form smaller radicals
- attack of H-abstrating radicals (O, OH, H, CH₃, C₂H₃, C₂H₅, HCO) and oxygen on RH
- alkyl radical R• decomposition
- olefin production from R• + O₂
- abstraction reactions from olefin by O, OH, H, CH₃
- olefin decomposition
- alkenyl radical decomposition

For the low-temperature oxidation of n-alkanes, the lumped reaction scheme, successfully used for n-C₇H₁₆, i-C₈H₁₈ and n-C₁₀H₂₂ combustion modeling [8, 10] has been applied. Due to the lack of experimental data for ignition delay times of n-C₁₆H₃₄, reactions of its low temperature oxidation chemistry have been omitted in the model.

Rates of reactions were carefully estimated by evaluating findings in the literature. Due to the lack of literature data the kinetic constants for heavy hydrocarbon reactions have been obtained from analogy with small molecules, also generic rates have been assigned to reactions of thermal decomposition, and to reactions of alkynes, allylic radicals, and other unsaturated species.

The kinetics parameters of the lumped reactions are derived from a linear lumping procedure and model optimization through minimizing the errors between predictions of oxidation products obtained by the detailed and the lumped kinetic model. Rates of lumped hydrogen abstraction and thermal decomposition reactions for isomers are adjusted in the pre-exponential factor to account for the number of all possible reactions according to the products. A rate of the controlling step by the cascading decomposition has been assigned to combined overall reactions.

The *n-propylcyclohexane* sub-mechanism is built as an extension of the *cyclohexane* (cyC₆H₁₂) sub-model, which has been first implemented in the core mechanism to represent chemistry of naphthenes. Equipped with all principal reactions and isomers analyzed in literature (see [12] for more detailed analysis) the cyclohexane sub-model has been reduced with the techniques described above to a skeletal scheme. The high temperature cyclohexane oxidation goes through decomposition of the cycloalkyl radical, cyC₆H₁₁, cascading dehydrogenation leading to benzene and smaller radicals, and the cyC₆H₁₁ ring-opening step. Reactions of the linear hexenyl radical isomerisation have been lumped. For low temperature cyC₆H₁₂ oxidation, the formation of intermediate species and transition states with 2 rings mark an important difference with respect to low temperature oxidation of linear hydrocarbons.

So, cyC₆H₁₁ reacts with O₂ to form only one type of a cycloperoxy (cyC₆H₁₁OO) radical leading to chain branching pathways, through

- isomerisation of cyC₆H₁₁OO through 4-, 5-, 6-, and 7-centres transition states (transition states with 2 rings) to form hydroperoxyalkyl (cyC₆H₁₀OOH) radicals
- isomerisation/decomposition of cyC₆H₁₀OOH radicals to linear hex-5-enal, cyclohexene, cyclohexanone, and three bicyclic ethers
- O₂ addition to cyC₆H₁₀OOH with formation O₂QOOH radicals
- isomerisation/decomposition of O₂QOOH to cyclic ketohydroperoxides, hydroxyl radical and different sets of products.

Table 3. Species pertaining to the n-propylcyclohexane oxidation sub – mechanism.

	cyC ₉ H ₁₈ , n-propylcyclohexane
	cyC ₉ H ₁₈ B, cyclohexyl-2-propyl
	cyC ₉ H ₁₈ E, 2-propyl - cyclohexyl
	cyC ₈ H ₁₅ , 2- cyclohexyl – ethyl
	cyC ₈ H ₁₄ , vinylcyclohexane
	cyC ₇ H ₁₃ , cyclohexyl – methyl
	cyC ₇ H ₁₂ , methylene cyclohexane

All three bicyclic ethers and cyclohexanone have been retained in the model, but hydroperoxyalkyl isomers have been lumped to one species. Concerning the reaction rates, it has been assumed that for the same reaction classes the rate constants are similar to those of normal alkanes. However, the ring strengths of the respective transition states are very different from those involved in the reaction of linear or branched peroxy radicals. Special care has been taken to evaluate the rate constants for the isomerization and the formation of cyclic ethers involved in bicyclic species formation. For some cyclohexane reaction rates (H-atom abstraction via HO₂, ring opening reaction and alkyl radical isomerization) experimentally measured or calculated values have been adopted [12].

The n-propylcyclohexane has been recently studied in several works [13, 25-27]. It was found that the parameters of thermal

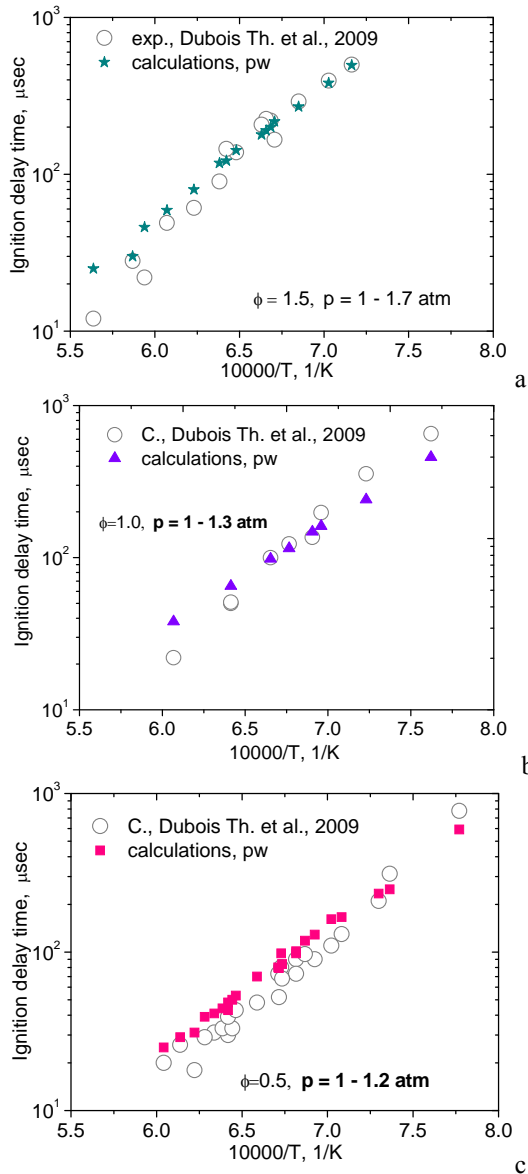


Figure 4. Comparison of modeled ignition delays for $\text{cyC}_9\text{H}_{18}/\text{air}$ mixtures with experimental data [13].

decomposition of mono-n-alkylcyclohexanes are functions of the length of the alkylic side chain. A comparison with analogous parameters of n-paraffins and the unsubstituted cyclohexane allowed the conclusion that C-C-scission in the alkylic chain is the initial reaction in pyrolysis of n-alkylcyclohexanes followed by radical attacks to all C-H-bonds of the feed molecules. In [25] the oxidation of n-propylcyclohexane has been studied in a jet-stirred reactor at atmospheric pressure over the temperature range 950-1250 K, and variable equivalence ratio ($0.5 < \phi < 1.5$). On this base a detailed kinetic reaction mechanism (176 species and 1369 reactions, most of them reversible) for n-propylcyclohexane oxidation at those conditions has been elaborated. The routes

involved in n-propylcyclohexane have been delineated: n-propylcyclohexane oxidation proceeds via H-atom abstraction forming seven distinct propyl-cyclohexyl radicals that react by β -scission yielding ethylene, propene, methylene-cyclohexane, cyclohexene, and 1-pentene. Kinetic data were derived from the literature analysis and analogy with small hydrocarbons and cyclohexane. In [27], the low-temperature autoignition of n-propylcyclohexane has been studied in a rapid compression machine over the pressure range 4.5-13.4 atm, between 620 and 930 K, and for three equivalence ratios $\phi = 0.3, 0.4$, and 0.5 . Two-stage ignitions are observed at the lowest pressures between 620 and 750 K. A negative temperature coefficient region is present at the lowest pressures for $\phi = 0.5$ and 0.4 .

The construction of the short n-propylcyclohexane oxidation sub-model is based on a mechanism proposed in [25]. This model was analyzed and reduced to a simplified description of the primary propagation reaction of the n-propylcyclohexane oxidation, which covers 7 new species, Table 3, involved in 51 successive oxidation and decomposition reaction classes for high temperature fuel consumption. These reactions yield linear species C_7H_{13} , C_5H_{10} , C_5H_9 , C_4H_7 , C_4H_6 , C_3H_7 , C_3H_6 , C_3H_5 , C_2H_4 , and cyclic $\text{cyC}_6\text{H}_{11}$, which already exist in reaction scheme.

Table 4. Low temperature lumped reactions for $\text{n-C}_{10}\text{H}_{22}$ and $\text{n-C}_{12}\text{H}_{26}$

Reaction rate is $k = A\alpha T^n e^{(-\frac{E}{T})}$, cm, mol, s, K.

Reactions	A	n	$\alpha_{\text{nC}_{10}\text{H}_{22}}$	$\alpha_{\text{nC}_{12}\text{H}_{26}}$	E
$\bullet\text{R} + \text{O}_2 = \text{RO}_2$	1.2E+19	-2.5	1	2.5	0
$\text{RO}_2 = \text{QOOH}$	2.0E+11	0	1	1	8500.0
$\text{QOOH} = \text{olefin} + \text{HO}_2$	2.0E+21	-2.5	1	1	11905.0
$\text{QOOH} = \text{olefin} + \text{aldehyde} + \text{OH}$	2.5E+13	0	1	1	11250.0
$\text{QOOH} + \text{O}_2 = \text{O}_2\text{QOOH}$	2.5E+12	0	1	1	0
$\text{O}_2\text{QOOH} = \text{OR}'\text{OOH} + \text{HO}$	1.5E+12	0	1	0	0
$\text{O}_2\text{QOOH} = \text{HOOR}'\text{OOH}$	2.0E+11	0	0	1	8500.0
$\text{HOOR}'\text{OOH} = \text{OR}'\text{OOH} + \text{HO}$	1.5E+12	0	0	1	0
$\text{OR}'\text{OOH} = \text{OR}'\text{O} + \text{HO}$	1.5E+12	0	0	1	0
$\text{O}_2\text{QO} = \text{decomposition}$	7.0E+14	0	1	0	21000.0
$\text{OR}'\text{O} = \text{decomposition}$	7.0E+14	0	0	1	21.0000

Although *n-dodecane* and *n-hexadecane* are a reference fuel for kerosene and diesel combustion only a limited number of kinetic studies of their gas-phase oxidation kinetics are available [15, 16, 28-30]. A detailed and reduced kinetic model for n-dodecane has been proposed in [28] for high temperatures. Most of the kinetics parameters for higher alkanes, alkyl radicals, and alkenes were estimated from analogy with reactions of n-butane, 1-butyl radical, and 1-butene, respectively. A modeling study of gas-phase oxidation

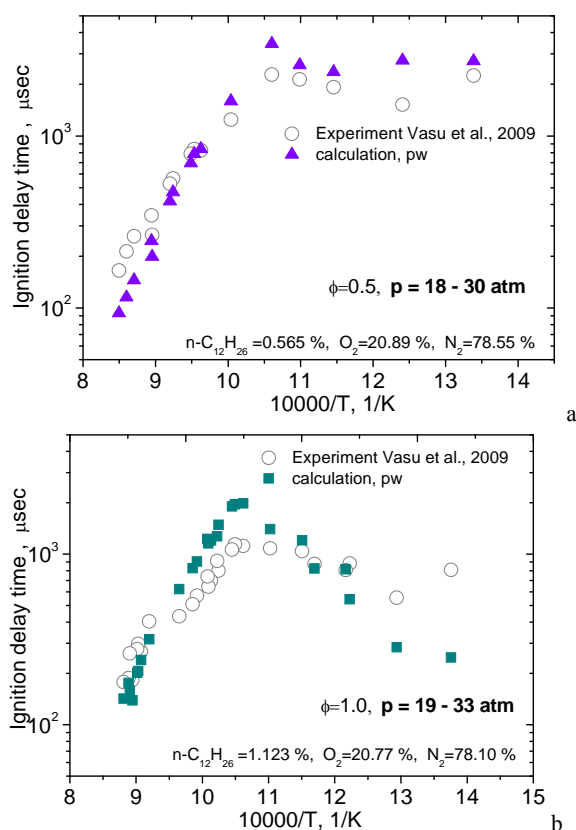


Figure 5. Comparison of modeled ignition delays for $n\text{-C}_{12}\text{H}_{26}/\text{air}$ mixtures with experimental data [14].

of n -hexadecane performed in a jet-stirred reactor at $p = 1.0$ atm, temperatures ranging from 1000 K to 1250 K and $\phi = 0.5$, 1, and 1.5 has been reported in [15]. The established kinetics model features 242 species and 1801 reactions and gives reasonable agreement with species profiles except for the parent fuel itself whose reactivity is underestimated. Semi-detailed sub-models for higher n -alkanes based on similarity of kinetic and oxidation behaviour of heavy and small n -alkanes at both high and low-temperature range have been elaborated in [27].

Kinetic parameters for different reaction classes involved in lumped oxidation reactions of large n -alkanes were evaluated. In the present work the n -dodecane and n -hexadecane lumped kinetic sub-models have been generated for the reaction classes described above. For n -dodecane, both high and low-temperature oxidation have been developed for 12 lumped species $\text{C}_{12}\text{H}_{25}$, $\text{C}_{12}\text{H}_{24}$, $\text{C}_{12}\text{H}_{23}$, $\text{C}_{12}\text{H}_{25}\text{O}_2$, $\text{C}_{12}\text{H}_{24}\text{OOH}$, $\text{OOC}_{12}\text{H}_{24}\text{OOH}$, $\text{HOOC}_{12}\text{H}_{23}\text{OOH}$, $\text{OC}_{12}\text{H}_{23}\text{O}$, $n\text{-C}_6\text{H}_{13}$, $\text{C}_4\text{H}_8\text{O}$, $n\text{-C}_8\text{H}_{17}$, $\text{OC}_{12}\text{H}_{23}\text{OOH}$ and for $n\text{-C}_{12}\text{H}_{26}$. The reaction types used for low temperature oxidation of large hydrocarbons in the mechanism are collected in Table 4. For high temperature oxidation of n -hexadecane only three components were introduced in the model, $n\text{C}_{16}\text{H}_{34}$, $\text{C}_{16}\text{H}_{33}$ and $\text{C}_{16}\text{H}_{32}$, which take place in high temperature reaction classes described above. Reaction rates in this model were evaluated from

analogy with reactions of n -heptane and n -decane, from [15, 29] and from lumping techniques applied to the detailed mechanism [15].

Reactions of the *1-methylnaphthalene* production and consumption have been developed early in the mechanism for the PAH formation [10]. In addition to the reactions of H-atom abstraction yielding the 1-naphthyl radical (A2-), the naphthylmethyl radical (A2CH_2) and naphthalene (A2) the following reactions of A2CH_3 consumption have been included in the present model:

- 1-methoxy naphthalene ($\text{A2CH}_2\text{OH}$) formation through OH addition to A2CH_2
- naphthaldehyde (A2CHO) formation in reactions of $\text{A2CH}_2\text{OH}$ and A2CH_2 with H, O, OH and O_2
- naphthoyl radical A2CO formation through A2CHO decomposition and reactions of H-abstraction from A2CHO with H, O, OH and O_2
- A2CO decomposition yielding A2-
- naphthoxy radical (A2O) formation through O, O_2 addition to A2- and naphthalene
- 1-naphthalenol (A2OH) formation through H-addition to A2O
- A2O and A2OH decomposition to A2 and indenyl

Reaction rates have been adopted from data outlined in [16,17]. The complete mechanism of 189 species and 1125 reactions and the associated thermochemical data are available from the corresponding author (nadja.slavinskaya@dlr.de).

NUMERICAL RESULTS AND DISCUSSION

In order to check the validity of the proposed reaction mechanisms, the ignition delay times for $\text{cyC}_9\text{H}_{18}/\text{O}_2/\text{Ar}$, $n\text{-C}_{12}\text{H}_{26}/\text{air}$, $\text{A2CH}_3/\text{air}$ and $\text{Jet-A}/\text{O}_2/\text{Ar}$ mixtures measured behind reflected shock waves [13, 14, 16, 18, 19] and concentrations of selected species under JSR conditions for $n\text{-C}_{16}\text{H}_{32}/\text{air}$ oxidation using data from [15], Table 2, were simulated using CHEMKIN II [31]. Thermodynamical properties follow from [32], literature data and calculated with

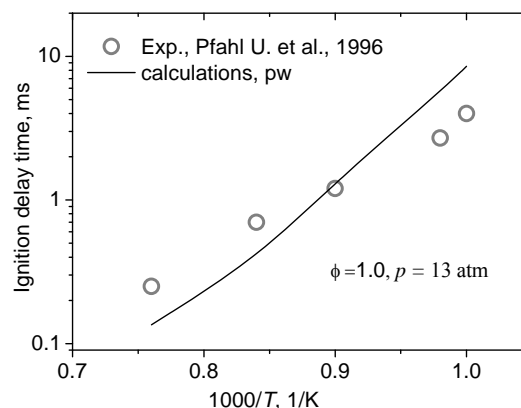


Figure 6. Comparison of modeled ignition delays for $\text{A2CH}_3/\text{air}$ mixtures with experimental data [16].

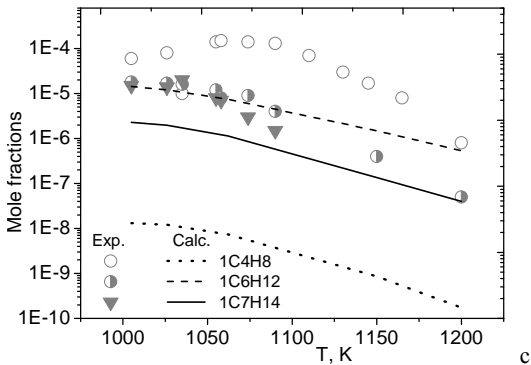
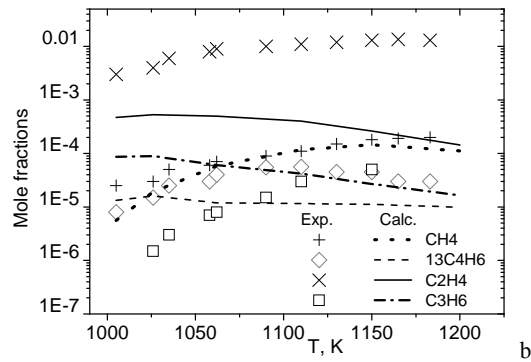
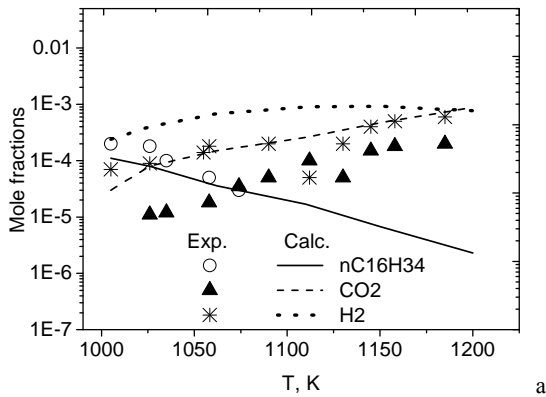


Figure 7. Experimental [14] (symbols) and computed (lines) mole fractions for the oxidation of n-hexadecane at 0.1 MPa in a JSR ($\phi = 1$, $\tau = 70$ ms). a) n-C₁₆H₃₄, CO₂, H₂; b) CH₄, 1,3C₄H₆, C₂H₄, C₃H₆; c) 1C₄H₈, C₆H₁₂, C₇H₁₄.

the Benson group additive method.

Ignition delay times of n-propylcyclohexane/O₂/Ar mixtures [13] were simulated for the following conditions: temperature range $T_0 = 1250$ – 1800 K, the pressure range $p = 1.0$ – 1.7 atm, and the equivalence ratio range $\phi = 0.2$ – 1.5 . As can be seen in Fig. 4, the model predicts the ignition delays fairly well yielding maximum discrepancies of less than a factor of two.

The n-dodecane sub-mechanism was validated on the ignition delay data [14] for the conditions $T_0 = 1250$ – 1800 K, $p = 18$ – 33 atm, $\phi = 0.5$, 1.0 , as shown in Fig. 5; experimental and simulation results agree reasonably well. Significant

discrepancies occur only at the lower temperatures. These discrepancies can be caused by some olefin intermediates not included in the model, which could be important for low-temperature combustion. Another possible reason for the discrepancies is the high level of uncertainty of the lumped reaction rates.

The predicted and measured [16] data for 1-methylnaphthalene ignition at $T_0 = 1000$ – 1335 K, $p = 13$ atm, and $\phi = 1.0$ are in good agreement, as shown in Fig. 6.

Due to the lack of experimental data for ignition delay times of n-C₁₆H₃₄, we had to use concentration data from the JSR experiment [15] for this sub-mechanism validation. Comparison of predicted and measured concentrations shows that although the decomposition of n-C₁₆H₃₄ concentrations of small molecules as H₂, CH₄, CO₂ and large olefins C₆H₁₂ and C₇H₁₄ are predicted quite well, Fig. 7a,c, concentrations of smaller olefins, such as C₂H₄, C₃H₆ and 1C₄H₈, reveal large discrepancies compared to measured data in both absolute value and trend, Fig. 7 b, c. The predicted concentration of ethylene is 7 times smaller than the experimental data at $T_0 = 1000$ K; this difference reaches 2 orders of magnitude at $T_0 = 1200$ K. The discrepancy for propene at $T_0 = 1000$ K and $T_0 = 1200$ K are 2 order of magnitude and a factor of 2, respectively; the discrepancy for 1C₄H₈ is 3 orders of magnitude for the overall temperature interval. The trends obtained for C₂H₄ and C₃H₆ indicate their over-consumption in

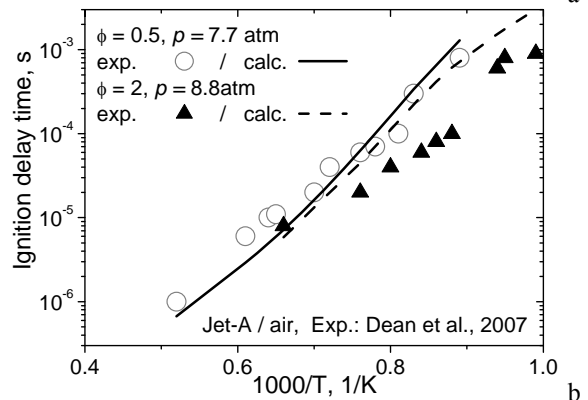
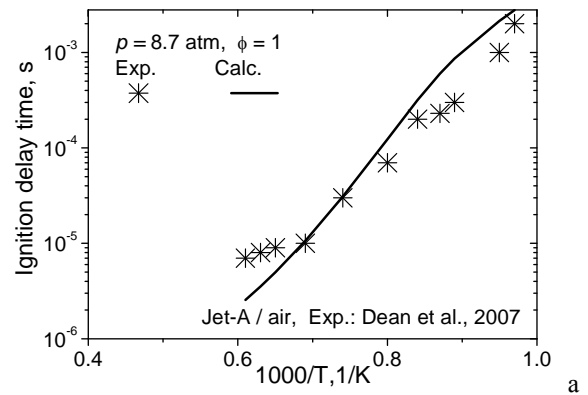


Figure 8. Comparison of modeled ignition delay times for Jet-A/O₂/Ar mixtures with experimental data [18] for $T_0 = 1010$ – 1929 K, $p = 7.7$ – 8.9 atm, and $\phi = 0.5$ – 2.0 .

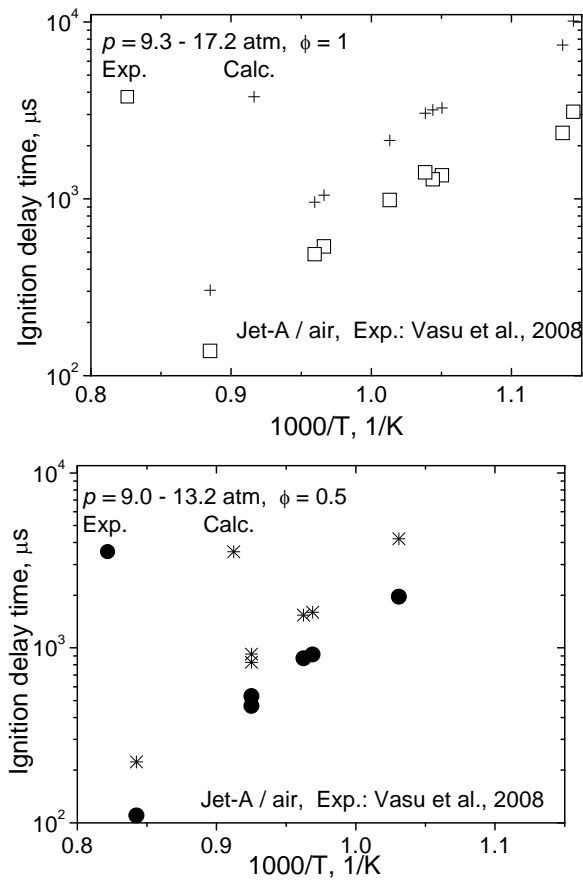


Figure 9. Comparison of modeled ignition delays for Jet-A/O₂/Ar mixtures with experimental data [19] for $T_0 = 874\text{--}1187\text{ K}$, $p = 19\text{--}25\text{ atm}$, and $\phi = 0.5\text{--}1.0$.

the model.

Thus, the short sub-model of n-C₁₆H₃₄ keeps the predictive capability for general features of fuel consumption, but the prediction of the interaction between small and large olefins needs to be improved. As the fuel consumption and concentration profiles of the main reaction products, i.e., CH₄, H₂, CO₂ are generally satisfactory reproduced, one can say, that the model reproduces the dynamic of fuel oxidation and can be used to describe the ignition delay time.

Based on these results of the stepwise validation of the reduced kerosene, the next step was to apply the mechanism to Jet-A ignition and to compare the predicted ignition delays with the results from [18 and 19], Fig. 8 and 9. The obtained agreement is good for the operating conditions $T_0 = 1010\text{--}1929\text{ K}$, $p = 7.7\text{--}8.9\text{ atm}$, and $\phi = 0.5\text{--}2.0$ [18], as seen in Fig. 8. The discrepancy for $T_0 = 874\text{--}1187\text{ K}$, $p = 19\text{--}25\text{ atm}$, and $\phi = 0.5\text{--}1.0$ [19] exceeds 2 times, as shown in Fig. 9. This discrepancy could be explained, first of all, with the absence of the low temperature sub-mechanism for n-hexadecane in the model and second, by the difference in combustion enthalpies

of the real fuel and the proposed surrogate, because the overprediction is observed for high temperature also.

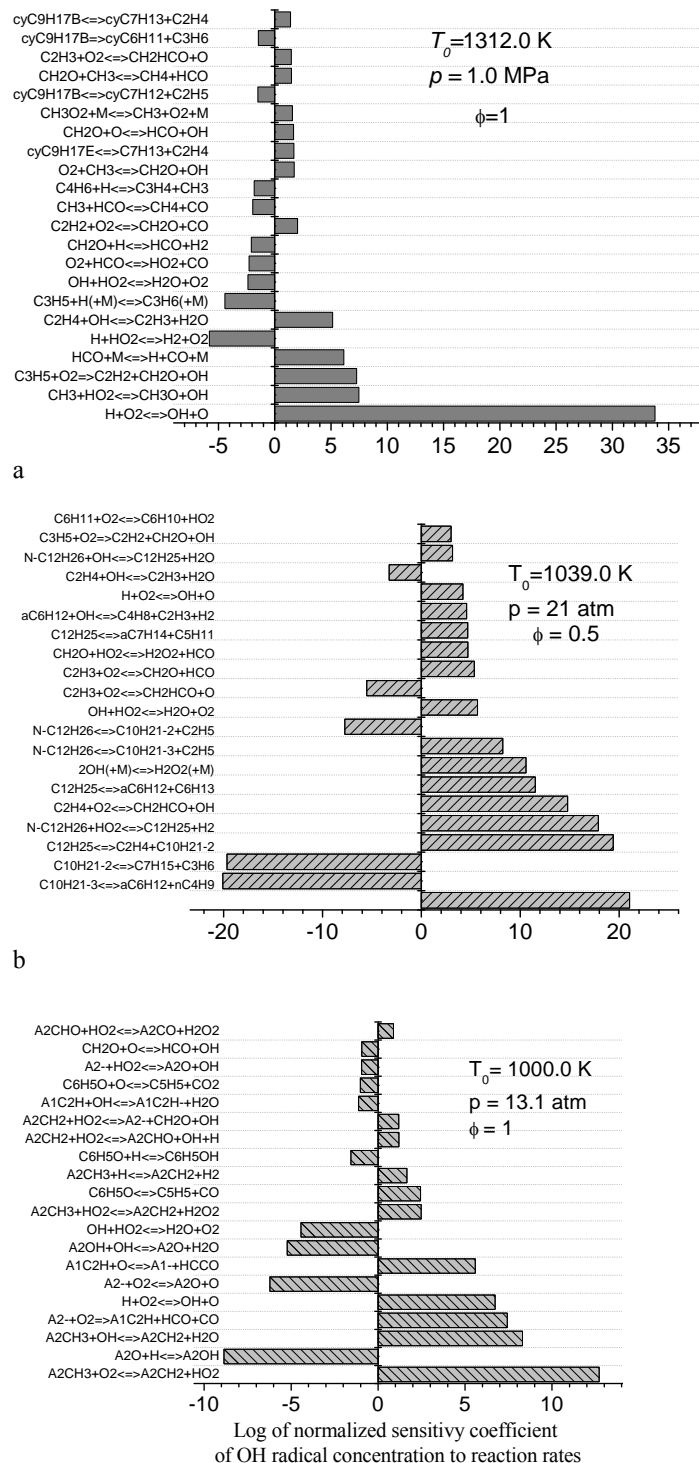


Figure 10. Logarithmical normalized sensitivity coefficients of the OH concentration to reaction rates for a) cyC₉H₁₈/air; b) n-C₁₂H₂₆/air; c) A2CH₃/air, 30% consumption of fuel.

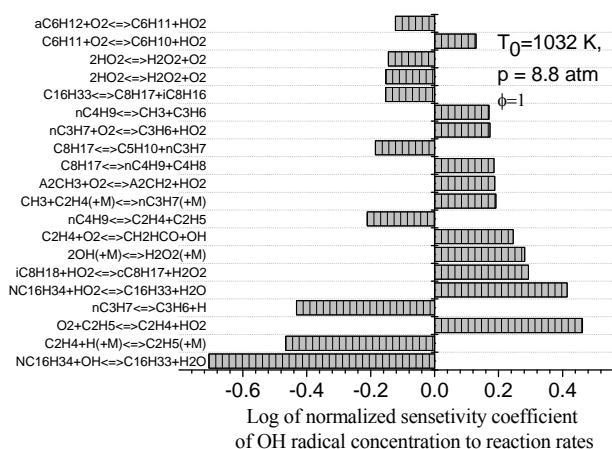


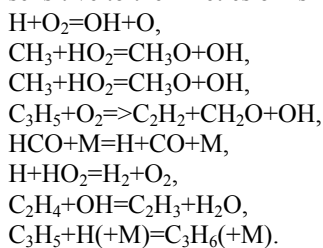
Figure 11. Logarithmical normalized sensitivity coefficients of the OH concentration to reaction rates for Jet-A/O₂/Ar. 30% consumption of fuel.

In any case, one can conclude, that surrogate blend obtained from optimization of physical properties of kerosene is able to reproduce the kerosene ignition delay as well.

Figures 10-13 summarize results of ignition delay sensitivity and rate of production analysis which have been performed for four mixtures: cyC₉H₁₈/O₂/Ar, n-C₁₂H₂₆/air, A2CH₃/air, and Jet-A/O₂/Ar at the time point of 30% of fuel consumption. Reactions with positive sensitivity coefficients promote the OH radical production whereas those with negative coefficients tend to consume OH.

The ignition of n-propylcyclohexane, Fig.10a, is mostly

sensitive to the kinetics of “small species chemistry”:



While decomposition reactions are the most important initial reactions of cyC₉H₁₈ consumption, alkylic side chain reactions are the dominant ones throughout the remaining oxidation.

Fig.10b shows that the n-dodecane decomposition and reactions of decyls and dodecyls, generated by H atom abstraction, dominate the OH production and consequently the ignition of n-C₁₂H₂₆/air mixture at the conditions studied. The analysis, Fig. 10c, reveals the H atom abstraction from 1-methylnaphthalene and subsequent A2- production as the most important initiation reactions for the A2CH₃/air mixture. However, further oxidation of A2- goes through two competing channels. The first forms A1 species and leads to further radical

production, and the second produces A2O that subsequently is converted into A2OH, which in turn consumes the important H radicals.

Finally, from the results of the sensitivity analysis, Fig. 11, for the surrogate mixture follows that reactions of the largest in proposed IFS hydrocarbon, n-C₁₆H₃₄, and reactions of the smallest olefins, C₂H₄ and C₃H₆, are the most effective for the OH production at kerosene ignition for the investigated conditions. The H-atom abstraction from n-C₁₆H₃₄ to form alkyl radical C₁₆H₃₃, which further decomposes into smaller alkyl and alkenes, dominates the process. Among the remaining four components of the surrogate, only i-C₈H₁₈ and A2CH₃ are of similar importance for H atom abstraction reactions that produce the appropriate alkyl radicals. From the results of the sensitivity analysis one can conclude that the process of mixture ignition is not a simple addition of reaction paths of individual components in the mixture. The competition between routes of oxidation of the initial hydrocarbons determines the radical pool in the system and the ignition chain reaction propagation. Reactions of ethylene and propene, which are known to be the most stable intermediate products in any oxidation reaction, are actively involved in the OH radical production in the investigated mixtures. In the reduced model these two species act as a link between large and small species in the surrogate. As it follows from analysis, Fig.11, not all species in IFS are equally important for ignition. Therefore based only on results of chemical properties analysis wrong conclusions can be done about the surrogate blend content. That can affect the ignition delay only slightly, but the model facility to reproduce physical properties becomes very

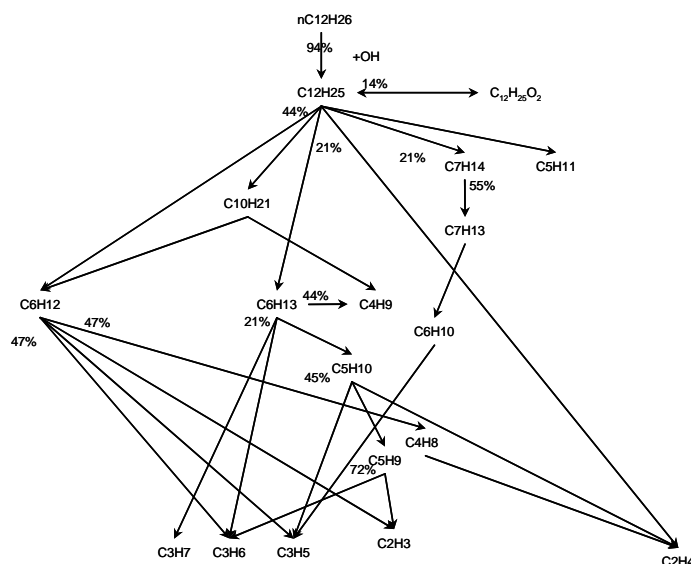


Figure 12. Primary reaction paths for the n – dodecane oxidation T₀ = 1039 K, p = 21 atm. Conversion 30%.

questionable. In other words, only multi-parameter optimization and multi-target reduction of the initial formula of

surrogate blend allows development of useful reference fuels. Studies of surrogate blends, as well as the development of numerical tools for fuel properties modeling are in progress at

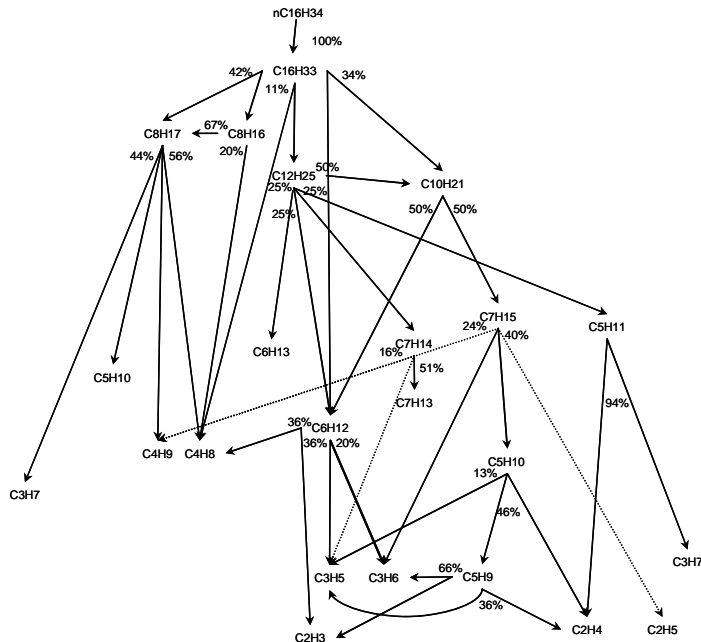


Figure 13. Primary reaction paths for the n – hexadecane oxidation in JSR , $\phi = 1$, $\tau = 70$ ms, 1000K.

our department and will contribute to a systematic understanding of all the dependencies in model fuel design.

Results of the reaction path analysis for autoignition conditions $T_0 = 1039$ K, $p = 21$ atm for n – dodecane and for n – hexadecane in a JSR at 1 atm, ($\phi = 1$, $\tau = 70$ ms, 1000 K) are presented in Fig.12 and 13. These figures highlight the main reaction routs and intermediates at fuel decompositions.

CONCLUSION

The ability to predict the chemical *and* physical properties of real fuels with a surrogate reaction model of manageable size is the major contribution of the present paper. The proposed process of reaction model design is based on optimization of the initial formula of the surrogate to mimic combustion enthalpy, formation enthalpy, molecular weight, C/H ratio, sooting tendency index, critical point, two-phase diagram, distillation curve, and ignition delay times. The resulting blend consists of 10% n-propylcyclohexane, 13% iso-octane, 20% n-dodecane, 23% 1-methylnaphthalene and 32% n-hexadecane and adequately represent the properties of kerosene (Jet-A).

In this paper the ignition delay times modeling and the elaboration of short reaction sub-models for n-propylcyclohexane, 1-methylnaphthalene, n-dodecane and n

-hexadecane have been described in detail. The applied simplifications in the construction process of sub-models has the aim to reduce the reaction pool to a set of reference

reactions and to restrict long-chained radicals and intermediate molecules directly to smaller radicals and molecules already existing in the compact core model. To achieve this, the following principles and methods have been used: neglecting of heavy radical reactions, use of a limited set of reference reactions, individual analysis of existing kinetics data, global sensitivity analysis, and chemical lumping.

The proposed sub-models were validated based on ignition delay data from shock tube experiments, and species concentrations measured in a jet-stirred reactor. Comparisons between experimental data and modeling results show that the elaborated semi-detailed kinetic models achieved reasonable agreement with the ignition and combustion data for n-propylcyclohexane, n-dodecane, 1-methylnaphthalene, n-hexadecane, and kerosene. But important discrepancies observed for the predictions of small alkenes by n-hexadecane oxidation in the JSR demonstrate that the lumped reaction rates for the olefin decomposition must be improved and the connection between the large molecule decomposition and small intermediate's production needs to be further investigated.

REFERENCES

- [1] Pitz, W. J., Cernansky, N. P., Dryer, F. L., Egolfopoulos, F. N., Farrell, J. T., Friend, D. G., and Pitsch, H., 2007, "Development of an Experimental Database and Chemical Kinetic Models for Surrogate Gasoline Fuels," SAE paper 2007-01-0175.
- [2] Colket, M., Edwards, T., Williams, S., et al., 2008, "Development of an Experimental Database and Kinetic Models for Surrogate Jet Fuels," 46th AIAA, Aerospace Sciences Meeting and Exhibit, Reno, Nevada, AIAA 2008-972.
- [3] Dagaut, P., Cathonnet, M., 2006, "The ignition, oxidation, and combustion of kerosene: A review of experimental and kinetic modeling," Progress in Energy and Combustion Science, 32, pp. 48–92.
- [4] Zhang, H. R., Eddings, E. G., Sarofim, A. F., 2007, "Criteria for selection of components for surrogates of natural gas and transportation fuels," Proc. Combust. Inst., 31, pp. 401–409.
- [5] Blanquart, G., Pepiot-Desjardins, P., Pitsch, H., 2009, "Chemical mechanism for high temperature combustion of engine relevant fuels with emphasis on soot precursors," Comb. and Flame, 156, 588–607.
- [6] Slavinskaya, N.A., Zizin, A., 2009, "On surrogate fuel formulation," ASME Turbo Expo 2009, Paper No GT2009-60012.
- [7] Edwards, T., Maurice, L.Q., 2001, "Surrogate mixtures to represent complex aviation and rocket fuels," Journal of Propulsion and Power, Vol. 17(2), pp. 461–466.
- [8] Slavinskaya, N.A., Haidn, O.J., 2003, "Modeling of n-heptane and iso-octane oxidation in air," J. Propul. Power, 19, pp. 1200–1216.
- [9] Slavinskaya, N.A., Frank, P., 2009, "A modelling study of aromatic soot precursors formation in laminar methane and ethene flames," Combust. Flame, 156, pp. 1705–1722.
- [10] Slavinskaya, N.A., 2008, "Skeletal mechanism for kerosene combustion with PAH production," 46th AIAA

Aerospace Sciences Meeting and Exhibit, Paper No AIAA 2008-0992.

- [11] Slavinskaya, N. A., Lenfers, C., "Skeletal Mechanism Production for n-Decane", 2nd Int. Workshop on Model Reduction in Reacting Flow, 2007, September 3-5, University of Rome "La Sapienza", Rome, Italy.
- [12] Slavinskaya, N.A., Wacker, M., Aigner, M., 2009, "Kinetic Modeling of Cyclohexane Oxidation with PAH Formation," Proc. Europ. Combust. Meeting.
- [13] Dubois, T., Chaumeix, N., Paillard, C.E., 2009, "Experimental and Modeling Study of n-Propylcyclohexane Oxidation under Engine-relevant Conditions," *Energy&Fuels*, 23, pp. 2453-2466.
- [14] Vasu, S.S., Davidson, D.F., Hong, Z., Vasudevan, V., Hanson, R.K., 2009, "n-Dodecane oxidation at high-pressures: Measurements of ignition delay times and OH concentration time-histories", *Proc. Combust. Inst.*, 32, pp. 173-180.
- [15] Ristori, A., Dagaut, P., Cathonnet, M., 2001, "The oxidation of n-Hexadecane: experimental and detailed kinetic modeling," *Combust. Flame*, 125, pp. 1128-1137.
- [16] Pfahl, U., Fieweger, K., Adomeit, G., 1996, "Self-ignition of diesel-relevant hydrocarbon-air mixtures under engine conditions," *Proc. Combust. Inst.*, 26, pp. 781-789.
- [17] Mati, K., Ristori, A., Pengloan, G., Dagaut, P., 2007, "Oxidation Of 1-Methylnaphthalene At 1-13 Atm: Experimental Study In A Jsr And Detailed Chemical Kinetic Modeling," *Combust. Sci. and Tech.*, 179, pp. 1261-1285.
- [18] Dean, A.J., Penyazkov, O.G., Sevruck, K.L., Varatharajan, B., 2007, "Autoignition of surrogate fuels at elevated temperatures and pressures," *Proc. Combust. Inst.*, 31, pp. 2481-2488.
- [19] Vasu, S.S., Davidson, D.F., Hanson, R.K., 2008, "Jet fuel ignition delay times: Shock tube experiments over wide conditions and surrogate model predictions," *Combust. Flame* 152, pp. 125-143.
- [20] Curran, H.J., Gaffuri, P., Pitz, W.J., Westbrook, C.K., 1998, "A Comprehensive Modeling Study of n-Heptane Oxidation," *Combust. Flame*, 114, pp. 149-177.
- [21] Warth, V., Stef, N., Glaude, P.A., Battin-Leclerc, F., Scacchi, G., Côme, G.M., 1998, "Computer-Aided Derivation of Gas-Phase Oxidation Mechanisms: Application to the Modeling of the Oxidation of n-Butane," *Combust. Flame*, 114, pp. 81-102.
- [22] Ranzi, E., Dente, M., Goldaniga, A., Bozzano, G., Faravelli, T., 2001, "Lumping procedures in detailed kinetic modeling of hydrocarbon mixtures," *Prog. Ener. Combust. Sci.*, 27, pp. 99-139.
- [23] Curran, H.J., Gaffuri, P., Pitz, W.J., Westbrook, C.K., 2002, "A comprehensive modeling study of iso-octane oxidation," *Combust. Flame*, 129, pp. 253-280.
- [24] Tomlin, A.S., Turányi, T., Pilling, M.J., 1997, "Mathematical tools for the construction, investigation and reduction of combustion mechanism," *Comprehensive chemical kinetics*, 35, pp. 293-437.
- [25] Ristori, A., Dagaut, P., El Bakali, A., Cathonnet, M., 2001, "The oxidation of N-propylcyclohexane: Experimental results and kinetic modeling," *Combust. Sci. and Technol.*, 165, pp. 197-228.
- [26] Matheu, D. M., Green, W.H., Grenda, J.M., 2003, "Capturing pressure-dependence in automated mechanism generation: Reactions through cycloalkyl intermediates," *Int. J. Chem. Kinet.*, 35, pp. 95-119.
- [27] Crochet, M., Vanhove, G., Ribaucour, M., Minetti R., 2009, "n-Propylcyclohexane lean oxidation and autoignition at low temperatures and elevated pressures", *Proc. Europ. Combust. Meeting*, 2009.
- [28] Ranzi, E., Frassoldati, A., Granata, S., Faravelli, T., 2005, "Wide-range kinetic modeling study of the pyrolysis, partial oxidation, and combustion of heavy n-alkanes," *Ind. Eng. Chem. Res.* 44, pp. 5170-5183.
- [29] Glaude, P.A., Battin-Leclerc, F., Fournet, R., Warth, V., Côme, G. M., Scacchi, G., Ristori, A., Pengloan, G., Dagaut, P., Cathonnet, M., 2001, "The gas-phase oxidation of n-hexadecane," *Int. J. Chem. Kinet.*, 33, pp. 574-586.
- [30] You, X., Egolfopoulos, F.N., Wang, H., 2009, "Detailed and simplified kinetic models of n-dodecane oxidation: The role of fuel cracking in aliphatic hydrocarbon combustion," *Proc. Combust. Inst.*, 32, pp. 403-410.
- [31] Kee, R.J., Rupley, F.M., Miller, J.A., 1993, "Chemkin-II: a FORTRAN chemical kinetics package for the analysis of gas phase chemical kinetics," Report No. SAND 89-8009B, Sandia Laboratories Report.
- [32] Burcat, A. Third Millennium Ideal Gas and Condensed Phase Thermochemical Database for Combustion, Technion Aerospace Engineering (TAE) Report # 867 January 2001, or "Burcat's Ideal Gas Thermochemical Database", <http://garfield.elte.chem/Burcat/burcat.html>.